

# Analytical and Numerical Study of Kramers' Exit Problem I \*

Alexander Spivak<sup>†</sup>, Zeev Schuss<sup>‡</sup>

Received 22 November 2001

## Abstract

Kramers' exit problem is concerned with noise activated escape from a potential well. In case the noise strength,  $\epsilon$ , is small this becomes a singular perturbation problem. The distribution of exit points on the separatrix (in the phase plane) is shown to be spread away from the saddle point, where the energy is minimal. The stochastic dynamics of the escaping trajectories, conditioned on not returning to a given critical energy contour, are studied analytically and numerically.

## 1 Introduction

Kramers' model of activated escape [1] has become a cornerstone in statistical physics with applications in many branches of science and mathematics [1]-[8]. It has important applications in diverse areas such as communications theory [4], stochastic stability of structures [6], and even in modern theory of finance [7]. Vast literature on exit problems has been accumulated [5] and the problem is still an active area of physical, chemical, biological, and mathematical research.

The purpose of this paper is to give a complete description of the exit distribution in the Kramers problem. This is achieved by mapping the exit distribution on the critical energy contour onto the separatrix, as found in [9], by means of the tails of the escaping trajectories. The tails, which are the trajectories of the original dynamics conditioned on reaching the separatrix before returning to the critical energy contour, obey different dynamics than the original trajectories.

Kramers' problem of activated escape [1] is concerned with the motion of a Brownian particle in a field of force. The motion is described by the dimensionless Langevin equation

$$\ddot{x} + \beta\dot{x} + U'(x) = \sqrt{2\epsilon\beta}\dot{w}, \quad (1)$$

where  $U(x)$  is a potential that forms a well with barrier height normalized to 1 (in the simulations is given by  $U(x) = 2x^4 - 1.2x^3 - 2x^2 + 1.45$ ),  $\beta$  is the dissipation constant, normalized by the frequency of vibration at the bottom of the well (in the simulations

---

\*Mathematics Subject Classifications: 60H10, 82C31, 46N55, 47N55.

<sup>†</sup>Department of Sciences, Academic Institute of Technology, POB 305, Holon 58102, Israel

<sup>‡</sup>Department of Mathematics, Tel-Aviv University, Tel-Aviv 69978, Israel

$\beta = 2$ ),  $\epsilon$  is dimensionless temperature (in the simulations  $\epsilon = 0.01$ ), normalized by the barrier height, and  $\dot{w}$  is standard Gaussian white noise [1]. If  $\epsilon$  is a small parameter (e.g., if the barrier of the well is high), the stochastic trajectories of eq.(1) stay inside the well for a long time, but ultimately escape [1]-[5]. To describe the escape process the Langevin equation is converted to the phase plane system

$$\begin{aligned} \dot{x} &= y \\ \dot{y} &= -\beta y - U'(x) + \sqrt{2\epsilon\beta} \dot{w}. \end{aligned} \tag{2}$$

The domain of attraction of the stable equilibrium point of the noiseless dynamics,

$$\begin{aligned} \dot{x} &= y \\ \dot{y} &= -\beta y - U'(x), \end{aligned} \tag{3}$$

located at the bottom of the potential well, is denoted by  $D$  and is bounded by a separatrix,  $\Gamma$ , which for small  $\epsilon$  is also the *stochastic separatrix* [8], that is, the locus of points where the random trajectories of (2) are equally likely to escape or to return to the well (see Figure 1.1 ). The specific exit problem for (2) is to determine the probability density function (pdf) of the points where escaping trajectories hit  $\Gamma$ .

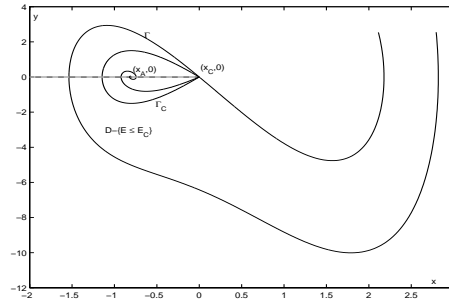


Fig 1.1. The domain of attraction  $D$  is bounded by the separatrix  $\Gamma$ . The domain  $D - \{E \leq E_C\}$  is bounded between  $\Gamma$  and by the critical energy contour  $\Gamma_C$ .

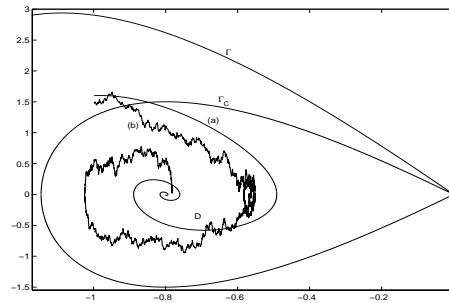


Fig. 1.2. A trajectory of the noiseless dynamics (3) and of the noisy dynamics (2) that start at a point between  $\Gamma_C$  and  $\Gamma$ .

Typically, when a trajectory of (2) crosses the critical energy contour  $\Gamma_C$ , defined by  $E = E_C$ , where

$$E = \frac{y^2}{2} + U(x), \quad E_C = U(x_C), \tag{4}$$

it is most likely to recross  $\Gamma_C$  and return to the neighborhood of the stable equilibrium point of the noiseless dynamics (3)  $(x_A, 0)$  (see Figure 1.2). Occasionally, a trajectory that crosses  $\Gamma_C$  goes on to cross  $\Gamma$  and escape the domain of attraction  $D$ . The part of an escaping trajectory from the last point where it hit  $\Gamma_C$  to the first point where it hits  $\Gamma$  is referred to as *the tail* of the escaping trajectory.

To investigate the problem of escape, we track the tails of the escaping trajectories. The stochastic dynamics of the tails is very different than that of the original system in the domain enclosed between  $\Gamma$  and  $\Gamma_C$  (compare Figures 1.2(b) and 3.1(b) below on page 4). Denoting by  $\tau_\Gamma$  the first passage time to  $\Gamma$  from any point  $(x, y)$  in that domain, and by  $\tau_C$  that to  $\Gamma_C$ , the dynamics of the tails is that of the original system (2) conditioned on hitting  $\Gamma$  before  $\Gamma_C$ , that is, on the event  $\tau_\Gamma < \tau_C$ . This conditioning modifies the drift of the tails by the logarithmic derivative of the probability

$$P(x, y) \equiv \mathbf{Pr}\{\tau_\Gamma < \tau_C \mid (x(0), y(0)) = (x, y)\}.$$

We study the modified dynamics in detail through the study of the function  $P(x, y)$ .

## 2 Notations and Formulation

The drift vector and the noise matrix of the stochastic system (2), corresponding to the Langevin equation (1) in the phase plane are denoted by

$$\mathbf{b}(x, y) = \begin{pmatrix} b_1(x, y) \\ b_2(x, y) \end{pmatrix} = \begin{pmatrix} y \\ -\beta y - U'(x) \end{pmatrix}, \quad \boldsymbol{\sigma}(x, y) = \begin{pmatrix} 0 & 0 \\ 0 & \sqrt{2\epsilon\beta} \end{pmatrix}. \quad (5)$$

The underlying deterministic dynamics of the system are governed by (3). Its phase plane portrait is given in Figure 1.1, where the point  $(x_A, 0)$  is an attractor, while the point  $(x_C, 0)$  is a saddle point. The domain of attraction of the attractor and its boundary are denoted by  $D$  and  $\Gamma$ , respectively. The curve  $\Gamma$  is the separatrix of the noiseless dynamics and in the limit  $\epsilon \rightarrow 0$  it becomes the stochastic separatrix. We denote by  $\omega_A = \sqrt{U''(x_A)}$  the frequency of oscillation at the bottom of the well, by  $\omega_C = \sqrt{-U''(x_C)}$  the imaginary frequency at the top of the barrier, and by  $E_C = U(x_C) - U(x_A)$  the critical energy measured from the bottom of the well, that is, the height of the barrier. In dimensionless units  $E_C = 1$ . We may assume that  $U(x_A) = 0$ . The contours of constant energy are given by (4). In particular, the critical energy contour, denoted by  $\Gamma_C$ , is given by  $E = E_C$ , or explicitly, by  $y = y_C(x) = \pm\sqrt{2[U(x_C) - U(x)]}$ . It is shown in Figures 1.1, 1.2, and 4.1.

The separatrix  $\Gamma$  is given by  $y = y_\Gamma(x)$ , where  $y_\Gamma(x)$  is the solution of the initial value problem [9]

$$y'_\Gamma(x) = -\beta - \frac{U'(x)}{y_\Gamma(x)}, \quad y_\Gamma(x_C) = 0. \quad (6)$$

Of the two solutions of (6),  $y_\Gamma(x)$  is the one with

$$y'_\Gamma(x_C) = -\frac{\beta + \sqrt{\beta^2 + 4\omega_C^2}}{2} = -\lambda. \quad (7)$$

We denote by

$$\boldsymbol{\nu}(x, y_\Gamma(x)) = \frac{1}{\sqrt{[\beta y_\Gamma(x) + U'(x)]^2 + y_\Gamma^2(x)}} \begin{pmatrix} \beta y_\Gamma(x) + U'(x) \\ y_\Gamma(x) \end{pmatrix} \quad (8)$$

the unit outer normal on  $\Gamma$ . At a point  $(x, y)$  near  $\Gamma$ , we denote by  $\boldsymbol{\nu}(x, y)$  the unit outer normal to  $\Gamma$  at the orthogonal projection of  $(x, y)$  on  $\Gamma$ .

We denote by  $\rho = \rho(x, y)$  the (signed) distance from the point  $(x, y)$  to  $\Gamma$ , such that  $\rho < 0$  in  $D$ , then

$$\nabla \rho(x, y) = \boldsymbol{\nu}(x, y) + O(\rho). \quad (9)$$

It follows from eqs.(5) and (8) that the vector  $\mathbf{b}(x, y_\Gamma(x))$  is tangent to  $\Gamma$ , that is,

$$\mathbf{b}(x, y_\Gamma(x)) \cdot \boldsymbol{\nu}(x, y_\Gamma(x)) = 0 \quad (10)$$

so that at points  $(x, y)$  near  $\Gamma$  the normal component of  $\mathbf{b}(x, y)$  is given by

$$\mathbf{b}(x, y) \cdot \boldsymbol{\nu}(x, y) = b_0(x)\rho(x, y) + O(\rho^2), \quad (11)$$

where the explicit form of  $b_0(x)$  is given in [9] as

$$b_0(x) = \frac{y_\Gamma(x)U'(x) - U''(x)(\beta y_\Gamma(x) + U'(x))}{y_\Gamma^2(x) + [\beta y_\Gamma(x) + U'(x)]^2}.$$

The pdf of the points where the stochastic trajectories of (2) hit the critical energy contour  $\Gamma_C$  for the first time, given that the trajectories started near the attractor, was calculated in [9]. It is given by

$$p_C(x) dx = \frac{[y_C(x) + o(1)] dx}{I_C} \quad \text{for } \epsilon \ll 1, \quad (12)$$

where  $I_C = \oint_{E=E_C} y_C(x) dx$  is the action of  $\Gamma_C$ . This means that the graph of  $p_C(x)$  is that of  $\Gamma_C$ , normalized by  $I_C$ . It is shown below that the pdf on constant energy contours close to  $\Gamma_C$  is close to (12).

Trajectories that start near the attractor and hit  $\Gamma$ , must cross the critical energy contour on their way to  $\Gamma$ . In particular, the part of an escaping trajectory between the *last* time it hit the critical energy contour and the *first* time it hits  $\Gamma$  (the *tail* of the trajectory) starts on the critical energy contour with the pdf  $p_C(x)$ . It follows that the tails map the exit pdf  $p_C(x)$  onto the exit pdf  $p_\Gamma(x)$  on  $\Gamma$ . We construct these tails approximately by first finding the pdf  $p_{\epsilon\delta}(x)$  on an energy contour  $\Gamma_{\epsilon\delta}$  close to  $\Gamma_C$  and then finding the dynamics of the tails that start on  $\Gamma_{\epsilon\delta}$  and reach  $\Gamma$  before  $\Gamma_C$ . These tails map  $p_{\epsilon\delta}(x)$  onto  $p_\Gamma(x)$ .

### 3 The Stochastic Dynamics of the Tails

The tails of the escaping trajectories form a new process, denoted by  $(x^*(t), y^*(t))$ , defined in the domain  $D - \{E \leq E_C\}$ , enclosed between  $\Gamma_C$  and  $\Gamma$ . The tails  $(x^*(t), y^*(t))$

are those trajectories of (2) for which  $\tau_\Gamma < \tau_C$ . The probability of the tails that start at  $(x, y) \in D - \{E \leq E_C\}$  is

$$P(x, y) \equiv \mathbf{Pr}\{\tau_\Gamma < \tau_C \mid (x(0), y(0)) = (x, y)\}.$$

The process  $(x^*(t), y^*(t))$  is a new diffusion process of the form

$$\begin{aligned} \dot{x}^*(t) &= y^*(t) \\ \dot{y}^*(t) &= -\beta y^*(t) - U'(x^*(t)) + 2\epsilon\beta \frac{\partial \log P(x^*(t), y^*(t))}{\partial y} + \sqrt{2\epsilon\beta} \dot{w}. \end{aligned} \quad (13)$$

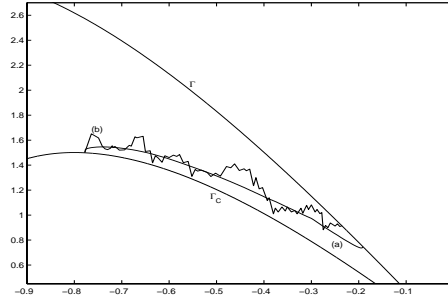


Fig. 3.1. Trajectories of the noiseless and noisy conditioned dynamics (13).

Note that the first component of  $\mathbf{b}^*(x, y)$  is the same as that of  $\mathbf{b}(x, y)$ , but the second component,  $b_2^*(x, y)$ , has the additional term  $2\epsilon\beta \partial \log P(x, y) / \partial y$ . The function  $P(x, y)$  is the solution of the backward Kolmogorov equation [2, 3]

$$\epsilon\beta \frac{\partial^2 P}{\partial y^2} + y \frac{\partial P}{\partial x} - [\beta y + U'(x)] \frac{\partial P}{\partial y} = 0 \quad (14)$$

in the domain  $D - \{E \leq E_C\}$ , with the boundary conditions

$$P(x, y_\Gamma(x)) = 1, \quad P(x, y_C(x)) = 0. \quad (15)$$

The boundary condition (15) is imposed on  $\Gamma_C$  and  $\Gamma$  for  $x < x_C$ . At  $x = x_C$  no boundary condition is assigned. This is a typical situation in boundary value problems with discontinuous boundary conditions.

Following [8], we transform  $P(x, y)$  to the form

$$P(x, y) = \sqrt{\frac{2}{\pi}} \int_{-\infty}^{\chi(x, y)/\sqrt{\epsilon}} e^{-z^2/2} dz,$$

where, according to eq.(14), the function  $\chi(x, y)$  satisfies the equation

$$y \frac{\partial \chi(x, y)}{\partial x} - [\beta y + U'(x)] \frac{\partial \chi(x, y)}{\partial y} = \beta \left[ \chi(x, y) \left( \frac{\partial \chi(x, y)}{\partial y} \right)^2 - \epsilon \frac{\partial^2 \chi(x, y)}{\partial y^2} \right]. \quad (16)$$

The boundary conditions for  $\chi(x, y)$  on  $\Gamma$  and  $\Gamma_C$  are  $\chi(x, y_\Gamma(x)) = 0$ ,  $\chi(x, y_C(x)) = 0$ , respectively. Obviously,

$$\chi(x, y) < 0 \quad (17)$$

for  $(x, y) \in D - \{E \leq E_C\}$ , outside a boundary layer.

The function  $\chi(x, y)$  can be expanded in a regular asymptotic power series away from  $\Gamma_C$ ,

$$\chi(x, y) = \chi_0(x, y) + \epsilon\chi_1(x, y) + \dots,$$

where  $\chi_0(x, y)$  satisfies the reduced equation (16), corresponding to  $\epsilon = 0$  and (17). According to [2, 8], for small  $\epsilon$ , the asymptotic approximation to  $P(x, y)$  outside a boundary layer near  $\Gamma_C$  is given by

$$P_0(x, y) = \sqrt{\frac{2}{\pi}} \int_{-\infty}^{\chi_0(x, y)/\sqrt{\epsilon}} e^{-z^2/2} dz. \quad (18)$$

To satisfy the second boundary condition (15), the approximation (18) has to be corrected by an additional boundary layer near  $\Gamma_C$ , as done below.

First, we describe the function  $\chi_0(x, y)$  near  $\Gamma$ . According to [9], inside the boundary layer region the function  $\chi_0(x, y)$  can be expanded in powers of the distance to the boundary. It can be written in the form

$$\chi_0(x, y) = \gamma(x)\rho(x, y) + O(\rho^2(x, y)), \quad (19)$$

where the function  $\gamma(x)$  is defined in [9] as the solution of the Bernoulli equation

$$y_\Gamma(x)\gamma'(x) + b_0(x)\gamma(x) = \beta\rho_y(x, y_\Gamma(x))\gamma^3(x)$$

where  $\gamma(x_C) = \sqrt{b_0(x_C)/\beta\rho_y^2(x_C, 0)}$ . If  $|\rho| < \epsilon$ , we have (near  $\Gamma$ )

$$\frac{\partial\chi_0(x, y)}{\partial y} \approx \frac{\partial\chi_0(x, y)}{\partial y} \Big|_\Gamma = \gamma(x) \frac{\partial\rho(x, y)}{\partial y} \Big|_\Gamma + O(\rho) \quad \text{for } |\rho| \leq \epsilon, \quad (20)$$

where the point  $(x, y)_\Gamma$  is the orthogonal projection of the point  $(x, y)$  on  $\Gamma$ , and

$$\sqrt{\frac{2}{\pi}} \int_{-\infty}^{\gamma(x)\rho(x, y)/\sqrt{\epsilon}} e^{-z^2/2} dz \approx 1 \quad \text{for } |\rho| \leq \epsilon.$$

Hence, inside the boundary layer,

$$\frac{\partial \log P(x, y)}{\partial y} = \frac{\partial P(x, y)/\partial y}{P(x, y)} \approx \frac{1}{\sqrt{\epsilon}} \frac{\partial\chi_0(x, y)}{\partial y} = \sqrt{\frac{1}{\epsilon}} \gamma(x) \frac{\partial\rho(x, y)}{\partial y} + O\left(\frac{\rho}{\sqrt{\epsilon}}\right). \quad (21)$$

To construct the dynamics of the tails in the domain  $D - \{E \leq E_C\}$ , the behavior of  $P(x, y)$  near  $\Gamma_C$  has to be determined. The conditioning on reaching  $\Gamma$  before  $\Gamma_C$  from any point in  $D - \{E \leq E_C\}$  renders the drift infinite on  $\Gamma_C$ . This can be seen from eqs.(13) and (15). Trajectories cannot be simply started on  $\Gamma_C$  and conditioned on reaching  $\Gamma$  before returning to  $\Gamma_C$ , because the drift of the tails is infinite on  $\Gamma_C$ . Rather, they can be started at any point with *energy higher* than  $E_C$  and conditioned on reaching  $\Gamma$  before  $\Gamma_C$ .

The asymptotic expansion of  $\partial \log P(x, y)/\partial y$  near  $\Gamma_C$  is constructed next. We correct the expansion (18) by constructing a boundary layer expansion of  $\partial \log P(x, y)/\partial y$

near  $\Gamma_C$ . First, we change the variables  $(x, y)$  to  $(x, E)$ , where  $E$  is the energy. The backward Kolmogorov equation (14) takes the form

$$y \frac{\partial P}{\partial x} + \beta (\epsilon - y^2) \frac{\partial P}{\partial E} + \epsilon \beta y^2 \frac{\partial^2 P}{\partial E^2} = 0.$$

Then, we introduce the stretched variable  $\zeta = (E - E_C)/\epsilon$  and expand  $P$  in powers of  $\epsilon$  to obtain the leading-order boundary layer equation

$$-\frac{\partial P^0}{\partial \zeta} + \frac{\partial^2 P^0}{\partial \zeta^2} = 0.$$

From here, with the help of (15), we obtain near  $\Gamma_C$

$$P^0(x, y) = C_\epsilon(x) (e^\zeta - 1) = C_\epsilon(x) \left( e^{\frac{E - E_C}{\epsilon}} - 1 \right),$$

where  $C_\epsilon(x)$  is independent of  $\zeta$ . This means that near  $\Gamma_C$

$$\frac{\partial \log P}{\partial y} \approx \frac{y}{\epsilon} \frac{e^\zeta}{e^\zeta - 1}. \quad (22)$$

The two expansions, (24) and (22), have to match near  $\Gamma_C$ , outside the boundary layer. Taking the limit  $\zeta \rightarrow \infty$  in (22), we obtain that the form of  $\chi_0(x, y)$  near  $y = y_C(x)$  must be such that

$$y_C(x) = -\chi_0(x, y_C(x)) \frac{\partial \chi_0(x, y_C(x))}{\partial y}.$$

Therefore the matched uniform expansion of  $\partial \log P / \partial y$  is given by

$$\frac{\partial \log P}{\partial y} = \frac{1}{P} \frac{\partial P}{\partial y} \approx \frac{1}{\sqrt{\epsilon}} \frac{\partial \chi_0}{\partial y} \frac{e^{-\chi_0^2/2\epsilon}}{\int_{-\infty}^{\chi_0/\sqrt{\epsilon}} e^{-z^2/2} dz} \frac{e^{\frac{E - E_C}{\epsilon}}}{e^{\frac{E - E_C}{\epsilon}} - 1}.$$

## 4 Asymptotic Analysis

In this section, we investigate the geometrical properties of the drift  $\mathbf{b}^*(x, y)$ . We show that the effect of conditioning is to “reverse” the drift in the sense that instead of drifting toward  $\Gamma_C$  it “points toward  $\Gamma$ ” everywhere in the domain  $D - \{E \leq E_C\}$ . To this end, we construct the function  $\chi_0(x, y)$  first inside a boundary layer near  $\Gamma$ , and then in  $D - \{E \leq E_C\}$ , outside the layer.

Using (21), we can write inside the boundary layer

$$b_2^*(x, y) \approx -\beta y - U'(x) + 2\sqrt{\epsilon} \beta \gamma(x) \frac{\partial \rho(x, y)}{\partial y}. \quad (23)$$

Outside the boundary layer, we have

$$\int_{-\infty}^{\chi_0(x, y)/\sqrt{\epsilon}} e^{-z^2/2} dz \approx -\frac{\sqrt{\epsilon} e^{-\chi_0^2(x, y)/2\epsilon}}{\chi_0(x, y)}, \quad \text{for} \quad \frac{-\chi_0(x, y)}{\sqrt{\epsilon}} \gg 1$$

(recall that  $\chi_0 < 0$  outside the boundary layer). Therefore, outside the layer,

$$\frac{\partial \log P(x, y)}{\partial y} \approx -\frac{1}{\epsilon} \chi_0(x, y) \frac{\partial \chi_0(x, y)}{\partial y} \quad (24)$$

and

$$b_2^*(x, y) \approx -\beta y - U'(x) - 2\beta \chi_0(x, y) \frac{\partial \chi_0(x, y)}{\partial y}. \quad (25)$$

Using (9) and (10) we obtain

$$\mathbf{b}^*(x, y_\Gamma(x)) \cdot \boldsymbol{\nu}(x, y_\Gamma(x)) = \sqrt{2\epsilon} \beta \gamma(x) \nu_2^2(x, y_\Gamma(x)) > 0. \quad (26)$$

Inequality (26) shows that the vector  $\mathbf{b}^*(x, y_\Gamma(x))$  forms an angle  $\theta$  with the normal  $\boldsymbol{\nu}(x, y_\Gamma(x))$  such that

$$\cos \theta = \frac{\sqrt{2\epsilon} \beta \gamma(x) \nu_2^2(x, y_\Gamma(x))}{|\mathbf{b}^*(x, y_\Gamma(x))|} > 0. \quad (27)$$

That is, the modified drift  $\mathbf{b}^*(x, y_\Gamma(x))$  points *away* from  $D$ . It follows that the deterministic trajectories  $\boldsymbol{\zeta}(t) = (\xi(t), \eta(t))$  of the modified drift,

$$\dot{\boldsymbol{\zeta}} = \mathbf{b}^*(\boldsymbol{\zeta}) \quad (28)$$

that start in  $D - \{E \leq E_C\}$  reach  $\Gamma$  in finite time, unlike the trajectories of the original drift

$$\dot{\boldsymbol{\zeta}} = \mathbf{b}(\boldsymbol{\zeta}), \quad (29)$$

which converge to the attractor as  $t \rightarrow \infty$ .

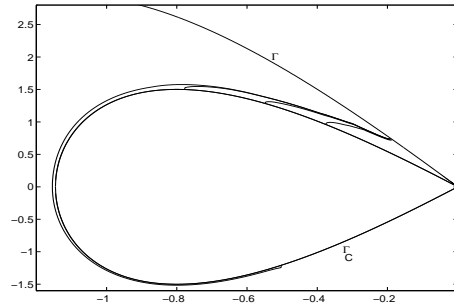


Fig. 4.1. Trajectories of (28) that begin near the part of  $\Gamma_C$  where most of the exit pdf is located, both for  $y > 0$  and  $y < 0$ .

Equations (23) and (25) determine the modified drift  $b_2^*(x, y)$  inside and outside the boundary layer near  $\Gamma$ . Near the critical energy contour  $\Gamma_C$  a separate expansion is needed, because the boundary condition (15) implies that  $P(x, y_C(x)) = 0$  so that  $b_2^*(x, y)$  becomes infinite, as described above.

As these trajectories reach the boundary layer near  $\Gamma$ , the drift becomes (23). A trajectory of (28) begins to curve in the direction of  $\Gamma$  at a distance  $\rho = \sqrt{\epsilon}/\gamma(x_C)$  from

$\Gamma$ . This is where we switch from the outer expansion of the modified dynamics (25) to the boundary layer expansion of (28), given by (23). Figure 3.1 shows a trajectory of the noiseless dynamics (28) and a typical trajectory of the noisy conditional dynamics (13) that starts at the same point near  $\Gamma_C$ . In Figure 4.1 trajectories of the noiseless conditiones dynamics are shown. In Figure 4.2 the behavior of the trajectories of the noiseless dynamics (13) that begin on  $\Gamma_C$  near the saddle point is given.

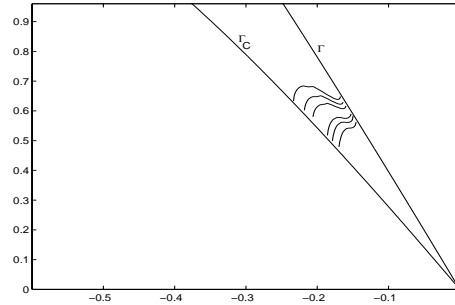


Fig. 4.2. A blow-up of the neighborhood of the saddle point.

## References

- [1] H. A. Kramers, Brownian motion in a field of force and the diffusion model of chemical reactions, *Physica (Utrecht)*, 7(1940), 284 -304.
- [2] Z. Schuss, *Theory and Applications of Stochastic Differential Equations*, John Wiley and Sons, New York, 1980.
- [3] C. W. Gardiner, *Handbook of Stochastic Methods*, Springer Verlag, N.Y. 1982.
- [4] B. Z. Bobrovsky and Z. Schuss, A singular perturbation method for the computation of the mean first passage time in a nonlinear filter, *SIAM J. Appl. Math.*, 42(1982), 174-187,
- [5] P. Hänggi, P. Talkner and M. Borkovec, 50 years after Kramers, *Rev. Mod. Phys.* 62(1990), 251-341.
- [6] A. Katz and Z. Schuss, Reliability of elastic structures driven by random loads, *SIAM J. Appl. Math* 45(3)(1985), 383-402 .
- [7] P. Wilmott, *Option Pricing: Mathematical Models and Computations*, American Educational Systems 1997.
- [8] D. Ryter, Noise-induced transitions in a double-well potential at low friction, *J. Stat. Phys.*, 49(1987), pp. 751-775.
- [9] B. J. Matkowsky, Z. Schuss and C. Tier, Uniform expansion of the transition rate in Kramers' problem, *J. Stat. Phys.*, 35(3/4)(1984), 443-456.